Available online at www.sciencedirect.com
ScienceDirect
Planetary and Space Science 54 (2006) 1298–1314
Planetary and Space Science
www.elsevier.com/locate/pss

The planetary fourier spectrometer (PFS) onboard the European Venus Express mission

V. Formisano[a,*], F. Angrilli[b], G. Arnold[c], S. Atreya[d], K.H. Baines[e], G. Bellucci[a], B. Bezard[m], F. Billebaud[i], D. Biondi[a], M.I. Blecka[g], L. Colangeli[p], L. Comolli[r], D. Crisp[o], M. D'Amore[a], T. Encrenaz[i], A. Ekonomov[f], F. Esposito[p], C. Fiorenza[a], S. Fonti[k], M. Giuranna[a], D. Grassi[a], B. Grieger[l], A. Grigoriev[f], J. Helbert[c], H. Hirsch[c], N. Ignatiev[f], A. Jurewicz[g], I. Khatuntsev[f], S. Lebonnois[m], E. Lellouch[i], A. Mattana[a], A. Maturilli[a], E. Mencarelli[a], M. Michalska[g], J. Lopez Moreno[j], B. Moshkin[f], F. Nespoli[a], Yu. Nikolsky[f], F. Nuccilli[a], P. Orleanski[g], E. Palomba[p], G. Piccioni[h], M. Rataj[g], G. Rinaldi[a], M. Rossi[a], B. Saggin[r], D. Stam[n], D. Titov[f], G. Visconti[q], L. Zasova[f]

[a]*Istituto di Fisica dello Spazio Interplanetario IFSI INAF, Via del Fosso de, l Cavaliere 100, 00133 Roma, Italia*
[b]*Universita' di Padova, CISAS, Via Venezia 1, 35131 Padova, Italy*
[c]*Deutsches Zentrum für Luft- und Raumfahrt e.V. (DLR) Optische Informationssysteme, Rutherfordstraße 2, 2439 Berlin, Germany*
[d]*College of Engineering, The University of Michigan, Space Research Building, 2455 Hayward Street, Ann Arbor, MI 43109-2143, USA*
[e]*Jet Propulsion Laboratory, MS 133-601, Pasadena, CA 91011, USA*
[f]*Space Research Institute of Russian Academy of Sciences (IKI), Profsojuznaja 34/32, 117997 Moscow, Russia*
[g]*Space Research Center of Polish Academy of Sciences (SRC PAS), Bartycka 13A, 00716 Warsaw, Poland*
[h]*Istituto Astrofisica Spaziale IASF INAF, Reparto di Planetologia, Via del Fosso del Cavaliere 100, 00133 Roma, Italia*
[i]*Observatoire de Paris Meudon, Department de Recherch Spatiale (DESPA),Place J.Janssen 5, 92195 Meudon, France*
[j]*Istituto de Astrofisica de Andalusia CSIC, P.O.B. 3004,13030 Granada, Spain*
[k]*Universita' degli Studi di Lecce, Dipartimento di Fisica, Via Arnesano, 73100 Lecce, Italy*
[l]*Max-Planck-Institute for Aeronomy, Max-Planck-Str. 2, D-37191 Katlenburg-Lindau, Germany*
[m]*LESIA, Observatoire de Paris, section de Meudon,Bât. 13, pièce 111, 92195 Meudon cedex, France*
[n]*Astronomical Institute "Anton Pannekoek", University of Amsterdam, Kruislaan 403, 1093 SJ Amsterdam, The Netherlands*
[o]*Jet Propulsion Laboratory,Earth and Space Sciences Division, Calfornia Institute of Technology, M/S 241-105, 4300 Oak Grove Drive, Pasadena, CA 91109-3099, USA*
[p]*Observatorio Astronomico di Capodimonte (OAC), Via Moiariello 16, 30131 Napoli, Italy*
[q]*Department of Physics, University of L'Aquila, Via Vetoio, 67010 L'Aquila, Italy*
[r]*Politecnico di Milano, Polo di Lecco,Via Marco D'Oggiono 13/A, 23900 Lecco, Italy*

Accepted 10 April 2006
Available online 26 September 2006

Abstract

The planetary fourier spectrometer (PFS) for the Venus Express mission is an infrared spectrometer optimized for atmospheric studies. This instrument has a short wavelength (SW) channel that covers the spectral range from 1700 to 11400 cm^{-1} (0.9–5.5 μm) and a long wavelength (LW) channel that covers 250–1700 cm^{-1} (5.5–45 μm). Both channels have a uniform spectral resolution of 1.3 cm^{-1}. The instrument field of view FOV is about 1.6 ° (FWHM) for the short wavelength channel and 2.8 ° for the LW channel which corresponds to a spatial resolution of 7 and 12 km when Venus is observed from an altitude of 250 km. PFS can provide unique data necessary to improve our knowledge not only of the atmospheric properties but also surface properties (temperature) and the surface-atmosphere interaction (volcanic activity).

PFS works primarily around the pericentre of the orbit, only occasionally observing Venus from larger distances. Each measurements takes 4.5 s, with a repetition time of 11.5 s. By working roughly 1.5 h around pericentre, a total of 460 measurements per orbit will be

*Corresponding author. Tel.: +39 06 49934362; fax: +39 06 49934074.
E-mail address: vittorio.formisano@ifsi.rm.cnr.it (V. Formisano).

0032-0633/$ - see front matter
doi:10.1016/j.pss.2006.04.033

acquired plus 60 for calibrations. PFS is able to take measurements at all local times, enabling the retrieval of atmospheric vertical temperature profiles on both the day and the night side.

The PFS measures a host of atmospheric and surface phenomena on Venus. These include the:(1) thermal surface flux at several wavelengths near 1 μm, with concurrent constraints on surface temperature and emissivity (indicative of composition); (2) the abundances of several highly-diagnostic trace molecular species; (3) atmospheric temperatures from 55 to 100 km altitude; (4) cloud opacities and cloud-tracked winds in the lower-level cloud layers near 50-km altitudes; (5) cloud top pressures of the uppermost haze/cloud region near 70–80 km altitude; and (6) oxygen airglow near the 100 km level. All of these will be observed repeatedly during the 500-day nominal mission of Venus Express to yield an increased understanding of meteorological, dynamical, photochemical, and thermo-chemical processes in the Venus atmosphere. Additionally, PFS will search for and characterize current volcanic activity through spatial and temporal anomalies in both the surface thermal flux and the abundances of volcanic trace species in the lower atmosphere.

Measurement of the 15 μm CO_2 band is very important. Its profile gives, by means of a complex temperature profile retrieval technique, the vertical pressure-temperature relation, basis of the global atmospheric study.

PFS is made of four modules called O, E, P and S being, respectively, the interferometer and proximity electronics, the digital control unit, the power supply and the pointing device.

Keywords: Venus; Planetary atmosphere; Spectroscopy

1. Introduction

Planetary fourier spectrometer (PFS) is included in the core scientific payload of the Venus Express. It is the key instrument in the study of the middle and lower atmosphere. It is inherited from the payload of ESA Mars Express mission but with some modifications conditioned by the particular properties of the Venus atmosphere and its radiation. PFS has two spectral channels, one for the long wavelengths (LWC, from 6 to 45 μm) and the second for the short wavelengths (SWC, from 0.9 to 6 μm). The spectral resolution is 1.3 cm^{-1} in both channels (see Formisano et al., 2005). Detailed instrument parameters are given in Table 1.

The aim of this paper is to overview briefly the scientific objectives and experiment performance at Venus. Scientific objective are given in Section 2, and a brief description of the experiment in Section 3.

Table 1
Summary of PFS–VEX parameters

Channel	SW	LW
Spectral range, μm cm^{-1}	0.9–6	6–45
	1700–11,400	220–1700
Spectral resolution, cm^{-1}	1.3	1.3
FOV, HW, rad	0.030	0.070
NEB, W cm^{-1} sr^{-1} cm^{-2}	$2\,10^{-10}$	310^{8}
Measurement cycle, s	11.5	11.5
Detector material	PbSe	$LiTaO_3$
Working temperature, K	200–220	290
Interferometer type	Double pendulum	
Reflecting elements	Cubic corner reflectors	
Beamsplitter	CaF_2	CsI
Maximal optical path difference, mm	±5	±5
Duration of the motion, s	4.5	4.5
Reference source	Laser diod	
Interferogram type	Two-sided	
Sampling number	22,500	4500
Sampling step, nm	450	1800
Dynamic range	$\pm 2^{15}$	

2. Scientific objectives

2.1. The atmosphere of Venus

The ratio of the mass of the Venus atmosphere to the mass of solid body is 10^{-4}, much more than in the case of the Earth and Mars. On the reference level (corresponding to the nominal surface radius 6052 km) the temperature is 735 K, and pressure of 92 bar. The most abundant atmospheric gas is CO_2. Its inventory is approximately the same as a total mass of carbonates on the Earth. The atmosphere contains also several percents of N_2. All other gases (see Section 2.8) are minor constituents. The water abundance is very low on Venus, it is an extremely dry planet. There are interesting peculiarities in the content of some other volatiles including noble gases.

A scheme of the vertical structure of the Venus atmosphere is presented in Fig. 1. Within the height range 0–55 km, the temperature lapse rate is nearly adiabatic, but between approximately 30 and 50 km it is a little lower than the adiabatic resulting in the formation of two convective zones separated by a stable region. The principal feature of atmospheric general circulation is the super-rotation with typical wind velocities of 60–120 m/s. The whole planet is covered by layers of clouds at heights of 49–70 km. However, a small but non-negligible part of the solar flux penetrates to the surface and heats the atmosphere due to the greenhouse effect. Venus has no intrinsic magnetic field and the solar wind interacts directly with the ionosphere. The upper atmosphere is relatively hot on the day side but very cold at night.

Not all is clear in this picture: very little is known about the general circulation of atmosphere below the clouds, its role in the planetary heat transfer, and about links between cloud structures and dynamics. Cloud particles in upper clouds consist mainly of sulphuric acid water solution; other condensates may exist, especially in middle and lower clouds. Possible role of volcanic events in the atmospheric processes is also far from being understood.

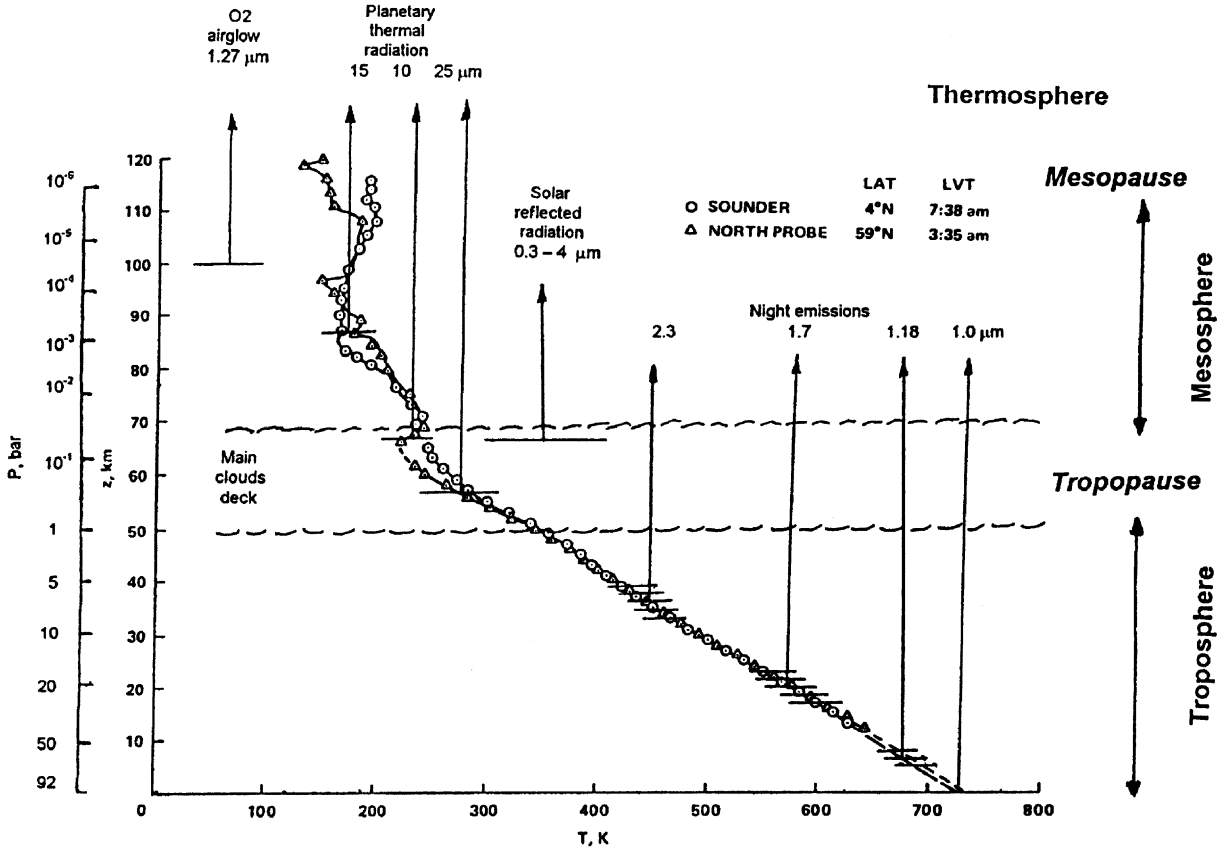

Fig. 1. The main elements of the vertical structure of the atmosphere of Venus. Circles and triangles present results of measurements of the temperature profile on two of four Pioneer probes (Seiff, 1983). They coincide within the troposphere, but there are differences in the mesosphere: inversions are observed at high latitudes and the low latitude profile is relatively smooth. Approximate positions of levels from which planetary radiation goes to space are shown.

At wavelengths shorter than approximately 3 μm, clouds of Venus attenuate radiation due to scattering rather than due to true absorption. By this reason some SW thermal radiation from deep hot atmospheric layers penetrates clouds in windows between CO_2 bands and goes to space. This radiation is negligibly small comparing with reflected solar radiation on the dayside, but it is well visible on the night side of Venus.

Fig. 1 shows also the approximate heights from which planetary thermal and solar reflected radiation leaves the planet at different wavelengths. This explains how observations of Venus in a wide spectral range provide a capability of the remote sounding of its atmosphere in the very wide range of heights. PFS–VEX experiment with its two channels: the LWC and the SWC is therefore an excellent tool for such a sounding.

Thermal infrared spectral measurements were made in the year 1983 with a Fourier spectrometer on board Venera 15 spacecraft (Moroz et al., 1986, Oertel et al., 1985, 1987). Examples of spectra obtained on Venera 15 are shown in Fig. 2. Spectral range of this instrument was 6–40 μm and spectral resolution 4.6–6.5 cm^{-1} with apodisation, spatial resolution near pericenter was 100 km. About 2000 high quality spectra were obtained, but the instrument failed after two months. The whole southern hemisphere and local times around noon and midnight were unexplored. Bands of H_2O and SO_2 in the thermal IR spectra of Venus were observed for the first time in this experiment (Zasova et al., 2004 and references therein).

Another important experiment was the orbiter infrared radiometer (OIR) (Taylor et al., 1980) of the Pioneer Venus Orbiter mission (1978). It had only several filters but their selection provided a capability of a rough but representative thermal and cloud structure sounding. The important discovery was that outgoing specific thermal flux in polar regions was larger than in the equatorial one.

Spectra of nightside of Venus are very interesting: they show a weak thermal emissions escaping from the atmosphere below the clouds in windows between the CO_2 bands and give information about abundances of the trace constituents in the lower atmosphere, their latitudinal, spatial, and time variations. This weak night thermal emissions were discovered by Earth based astronomical observations (Allen and Crawford, 1984), and observed later with high spectral resolution. The thermal radiation from the surface dominates in 1-μm night emission (Meadows and Crisp, 1996; Baines et al., 2000).

There is also an interesting NIR emission that comes from the upper atmosphere: O_2 $^1\Delta$ airglow at 1.27 μm (Connes et al., 1979), observable both on the night side and

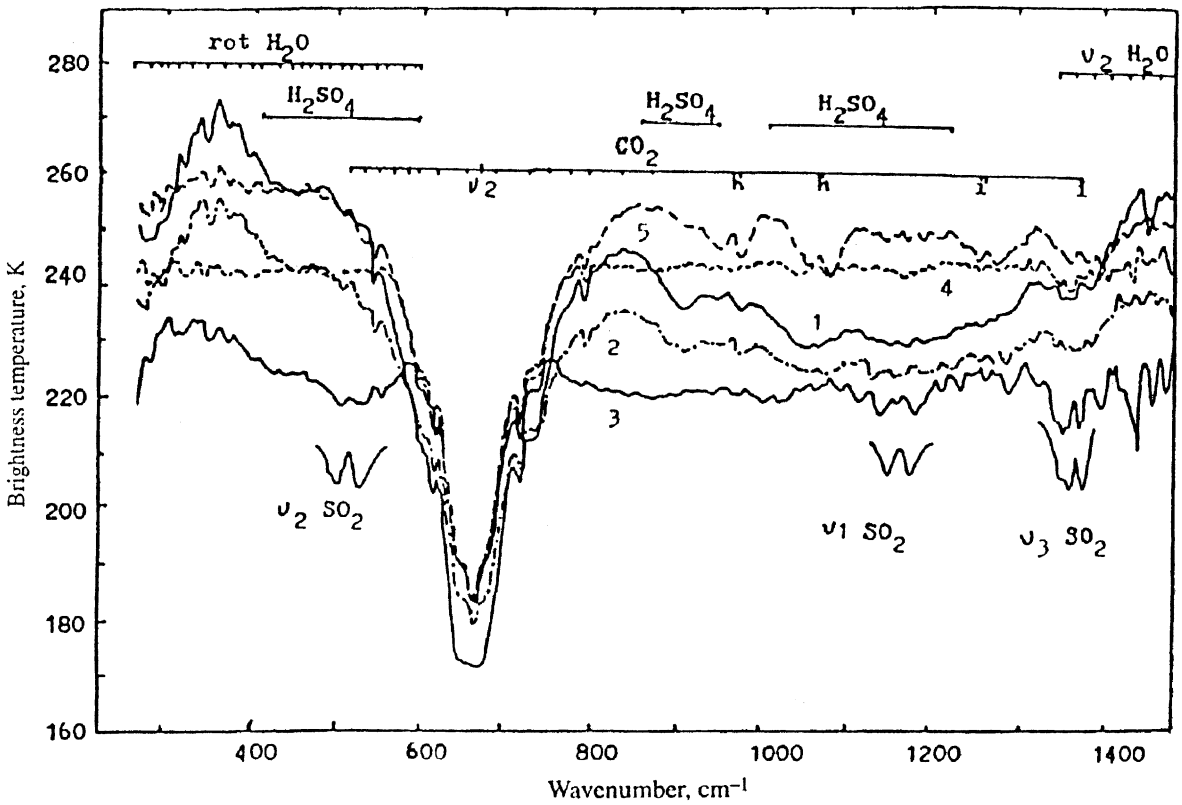

Fig. 2. Examples of spectra obtained by means of Fourier spectrometer of Venera 15. It covered approximately the same spectral range, as PFS–VEX LWC but had lower spectral resolution. These are averaged (from 5 to 10 individual) spectra for different latitudinal zones: equatorial (1); mid-latitude, $\varphi < 59$ (2); high-latitude ($60 < \varphi < 80$) from "cold collar" (3); polar region, usually $\varphi > 85$ (4); hot dipole structure in high latitudes (5).

on the dayside of the planet. Its source is the recombination of O atoms produced on the Venus dayside, mostly at 100–120 km. They are transported by the global circulation to the night side.

2.2. PFS–VEX goals

The Venus Express mission focuses on the global investigation of the atmosphere and soil. The PFS–VEX experiment will provide basic new data about characteristics of the Venus climate and atmosphere that will be important for studying some important basic problems, namely:

PFS LW channel

- Long-term global 3-D measurements of the temperature field in 55–100 km altitude range.
- Subsequent determination of zonal and meridional components of the wind in the altitude range 55–100 km.
- Monitoring of the upper cloud structure and composition,
- Measurements of abundance of SO_2, H_2O at 60–75 km altitude,
- Measurements of the outgoing thermal spectral fluxes (radiative balance),
- Investigation of the thermal tides and periodicities in the temperature and zonal wind fields, in the upper clouds and possibly in the abundance of minor compounds.

PFS SW channel

Day side observations:

- Optical properties of the upper clouds. Determination of the optical properties of the upper clouds from the observations at different zenith and phase angles.
- Mixing ratio of minor compounds (H_2O, SO_2, CO, HCl, HF) in the atmosphere above the clouds and near the cloud tops.
- Monitoring of the airglow emission of the O_2 $^1\Delta$ ro-vibrational band at 1.27 μm.

Night side observations

- Study of the atmospheric composition (CO, COS, H_2O, SO_2, HCl) below the clouds.
- Study of the cloud opacity and its variations.
- Measurements of the temperature gradient at 0–10 km and the surface temperature.
- Search for volcanic activity.
- Thermal mapping and monitoring of the surface in the 1 μm windows region.
- Monitoring of the airglow emission of the O_2 $^1\Delta$ ro-vibrational band at 1.27 μm.

Figs. 3–5 present synthetic spectra of Venus in the range of PFS sensitivity. The spectrum of Venus outgoing

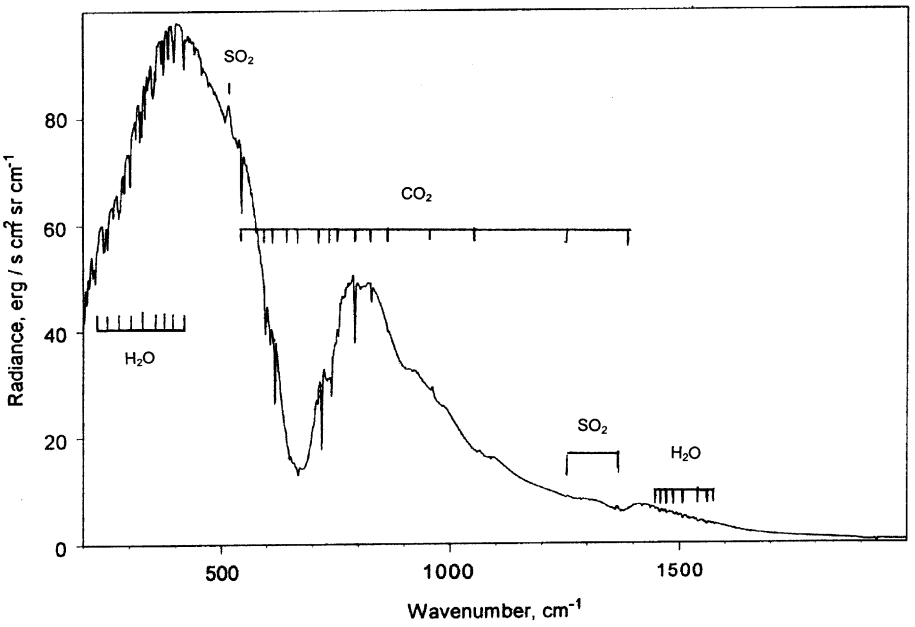

Fig. 3. Venus synthetic PFS LWC spectrum. It is practically the same on the day and night side of the planet. If presented in terms of brightness temperature, the spectrum would be similar to that measured by Venera 15 shown in figure 2.3.1 but with about 3 times better spectral resolution.

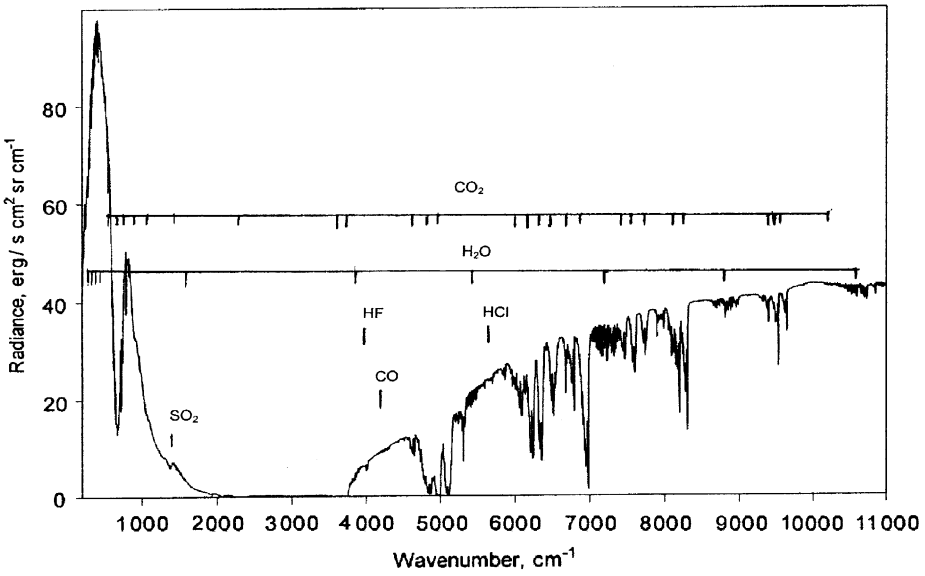

Fig. 4. Venus synthetic PFS spectra for the day side of the planet. SWC range starts from 2000 cm^{-1} (5 μm).

radiation (as that of every planet) consists of two main parts: the solar reflected radiation and planetary thermal radiation. The boundary between both is near 2500 cm^{-1} (4 μm) for the dayside. All pronounced spectral features are CO_2 bands. There are many other spectral features that belong to minor constituents like CO, H_2O, etc. and can be used to estimate their abundances at different altitudes.

The shape of the LWC spectra is governed by the following factors:

(1) temperature profile;
(2) aerosol vertical profile, which defines the level of formation of radiation outside of the gaseous absorption bands;
(3) vertical profile and mixing ratios of the absorbing gases. Among them there are CO_2, the main constituent, and two minor: H_2O and SO_2.

The most pronounced CO_2 spectral feature is the 667 cm^{-1} (15 μm) fundamental band. Other CO_2 features of special interest are 961 and 1064 cm^{-1} hot bands, and 1259 and 1366 cm^{-1} isotopic ($^{12}C^{16}O^{18}O$) ones.

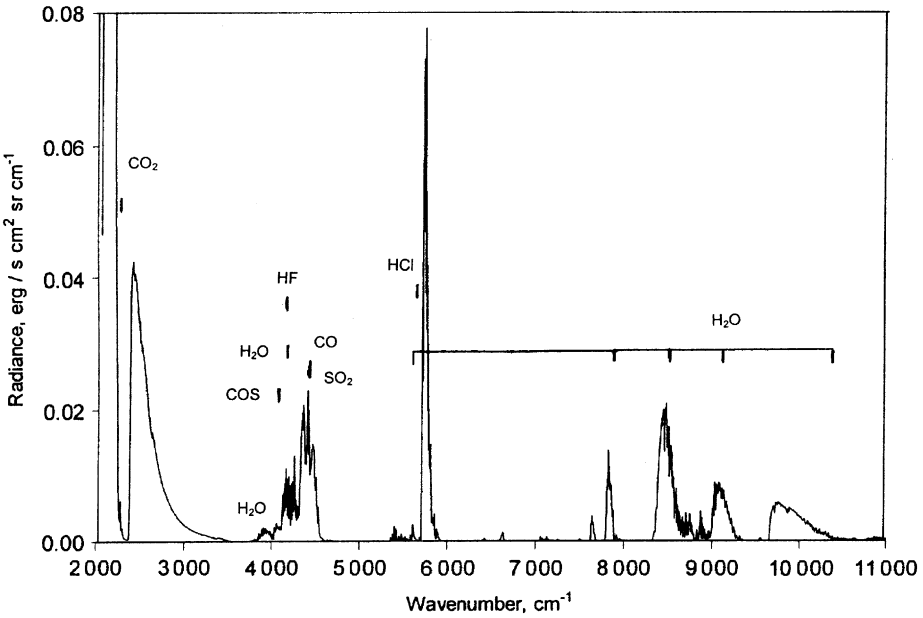

Fig. 5. Venus synthetic PFS SWC spectrum for the night side of the planet.

H_2O is visible in two parts of the LW channel spectrum: 280–475 cm^{-1} rotational band; 1590 cm^{-1} (6.3 μm) roto - vibrational fundamental band.

There are three bands of SO_2: v_2 (519 cm^{-1}), v_1 (1150 cm^{-1}) and v_3 (1360 cm^{-1}).

Some features belong to the liquid sulfuric acid: 450, 580, 900, 1150 cm^{-1} (the 580 cm^{-1} feature is in the wing of the 667 cm^{-1} CO_2 band).

The shape of the SWC spectra of the day side of the planet is governed by:

(1) multiple scattering of the solar radiation by particle clouds dominating above approximately $>4000\,cm^{-1}$;
(2) true absorption of the solar radiation by the liquid H_2SO_4 in clouds' particles, dominating below $<4000\,cm^{-1}$;
(3) abundances of absorbing gases (CO_2, H_2O, CO, HCl, HF) within and above upper clouds. CO_2 features are dominating everywhere. H_2O, CO bands are much weaker, but clearly visible. HCl, and HF are very weak, but possibly may be observed with PFS spectral resolution.

The shape of the SWC spectra of the night side of the planet is determined by the following factors:

(1) temperature profile;
(2) vertical profile and mixing ratios of the absorbing gases, namely the main compound CO_2 and several minor constituents H_2O, SO_2, CO, OCS, HCl, HF. Their spectral features are observable in the "windows" between much stronger CO_2 bands;
(3) attenuation of radiation by the clouds (for $v>3500\,cm^{-1}$);
(4) thermal radiation of the clouds (for $v<3500\,cm^{-1}$);
(5) thermal radiation of the surface (near 10,000 cm^{-1}).

The fundamental v_3 CO_2 band near 2349 cm^{-1} is observable both in night and day side spectra but in the latter case its formation is more complicate due to superposition of the thermal and solar scattering radiation.

More detailed discussion of the PFS–VEX scientific goals is given in Sections 2.5–2.12.

2.3. Temperature/aerosol retrieval

Temperature and aerosol vertical profiles will be retrieved in a self-consistent way from the same spectrum. Extinction cross-section of sulphuric acid particle in the thermal IR spectral range changes up to 30 times, depending on particle size. The spectral regions where maximum (at 1150 cm^{-1}) and minimum (at 365 cm^{-1}) of extinction coefficient occur are free from gas absorption and may be used for aerosol retrieval. For the case of PFS–VEX the minor constituents (as SO_2 and H_2O) could be also included in the self-consistent procedure.

Temperature retrieval from IR spectrum is an inverse problem for transfer equation. For planetary atmospheres, two classes of methods are most frequently used: Chahine relaxation method and its modifications and statistical regularization methods. Both of them were used at the first steps of the work on the temperature retrieval (in approximation of pure gaseous atmosphere) from Venera15 data (Spankuch et al., 1985), however, it was found

later that the used modification of relaxation method (Twomay et al., 1977) works more effectively for the case of the self-consistent temperature and aerosol retrieval. Description of the relaxation method for self-consistent temperature and aerosol retrieval can be found in Zasova et al. (1999).

PFS–VEX will provide important progress in studies of clouds combining capabilities provided by three modes of observations: with LWC (like Venera 15), with SWC night (like Galileo) and SWC day (ones realized earlier on Venera 9, but with very low spectral resolution). SWC day measurements of CO_2 bands will give direct and reliable estimates of altitude of boundary of upper clouds at high latitudes where aerosol scale height is small (in the absence of a haze, which may be transparent in the thermal IR, but ifluences the NIR spectrum). At latitudes below 55° interpretation will be more complicated. Here the scattering coefficient in upper clouds may be obtained from CO_2 daily SW bands measurements using aerosols scale height taken from the thermal IR.

PFS–VEX will advance our possibility of wind observation, including better coverage in space and local time. Higher spectral resolution will help to obtain more accurate temperature profiles, especially at high levels in the atmosphere, and more accurate wind field, possibly both zonal and meridional components. Monitoring of the cloud features in the SWC will give some information about wind speed in the cloud deck.

2.4. Minor constituents

Information about minor constituents that were identified in the atmosphere of Venus and could be measured with IR spectrometers is presented in Table 2. All of them may be observed by PFS–VEX. Positions of corresponding spectral bands are shown in Figs. 3–5.

Table 2 starts from H_2O and SO_2. These two molecules are especially interesting by two reasons: (1) both of them are greenhouse gases; (2) both participate in the cloud chemistry. PFS may measure them within and above the upper clouds (LWC and SWC) as well as in lower atmosphere (SWC, night emissions). Both of them show strong variability (with altitude and latitude) that will be important subject for PFS observations.

CO in the lower atmosphere demonstrates no or little altitude variability, but some variations with latitude were observed and interpreted as dynamical tracers (Taylor et al., 1997).

COS should participate in sulphur chemistry. It was observed only from the Earth with very high resolution in night emission. There is no information about latitudinal dependence. Possibly it may be obtained by PFS, but it will be a difficult task.

HCl and HF mixing ratios are very low, and their observations are also difficult. These gases may be related to volcanic eruptions. So their place-to-place variations (if exist) may say something about volcanoes on Venus.

Table 2
Minor constituents identified in the atmosphere of Venus (except of noble gases)

Molecule	Mixing ratio, ppm	Altitude, km	References	Comments
H_2O	30–40	0–40	1–4	NIR night emissions and optical spectrometry on Venera 11,13,14
	2–30	58–62	5	Thermal IR, FS on Venera 15
D/H	120 ± 40 terr	65–70	6	Day side reflection spectrum
SO_2	130 ± 35	<42	7	Venera 12 Chromatograph
	120 ± 20	42	8	Vega 1, 2, UV on probe
	30–40	22	8	Vega 1, 2, UV on probe
	130 ± 40	35–45	9	Night emissions
	1×10^{-6}–1.0	69	10	Thermal IR, FS of Venera 15
CO	23 ± 7	30	1, 9	Night emissions
	29 ± 7	40	1, 9	
			11	Day side reflection spectrum
COS	0.35 ± 0.1	30	1, 9	Night emissions
HCl	0.5 ± 0.15	15–30	9	Night emissions
		65–70	12	Day side reflection spectrum
HF	0.005 ± 0.002	30–40	9	Night emissions
		65–70	12	Day side reflection spectrum
H_2SO_4	11–20	40	13	13 cm radio occultations (gas phase below clouds; condensed phase in upper clouds shows a broad continuum and diffuse bands absorptions)

References: (1) Pollack et al. (1993); (2) de Bergh et al. (1995, 1998); (3) Meadows and Crisp, (1996); (4) Ignatiev et al. (1997); (5) Ignatiev et al. (1999); (6) de Bergh et al. (1991); (7) Gelman et al. (1979); (8) Bertaux J.-L. et al. (1996. p. 2) (9) Bezard et al. (1993); (9) Bezard, (1994); (10) Zasova et al. (1993), (11) Connes et al. (1968); (12) Connes et al. (1967); (13) Jenkins and Steffes, (1991,1994).

Estimates of upper limits for gases that were not identified in the atmosphere of Venus are published in several sources (Moroz, 1981; von Zahn et al., 1983, von Zahn and Moroz, 1985). Lists of these gases include O_3, C_3O_2, CH_4, C_2H_2, C_2H_4, H_2S, N_2O, NO_2 and many others that have absorption features in the PFS range. Corresponding upper limits are low ($<10^{-3}$ ppm) but PFS could provide in many cases even lower new values. Some of upper limits might be replaced by positive identifications due to PFS observations. It should be noted that these studies will not be limited to the dayside of Venus, but will possibly be extended to the night side as PFS will also cover rather well the night side of Venus atmosphere.

More specifically, PFS exploits seven atmospheric windows between 0.85 and 2.5 μm observed on Venus' nightside to sample the lower atmosphere and surface. Within the 1.7 and 2.3 μm windows, the spectra can be analyzed to infer the abundances of several key trace gases, including H_2O, SO_2, CO, OCS, and HCl at levels between the base of the main cloud layer (~47 km) and the surface (c.f. Crisp et al., 1989, 1991, Bézard et al., 1990; Grinspoon et al., 1993; Pollack et al., 1993). The intensity at wavelengths outside of the gas absorption bands provides information about the opacity and vertical distribution of the clouds. The spatial patterns mapped by PFS utilizing spacecraft scanning techniques gives motions of cloud layers at 50 and 57 km altitude, which appear silhouetted against the warmer layers below, as shown in. The radiation measured in five atmospheric windows between 0.8 and 1.2 μm originates primarily at the surface. Observations in these windows provide information about the surface temperature, surface emissivity, and near-surface thermal structure (Meadows and Crisp, 1996). These windows have been observed previously by the flyby observations of the Galileo/near-infrared mapping spectrometer (NIMS; Carlson et al., 1991, 1993) and the Cassini/visible and infrared mapping spectrometer (VIMS; Baines et al., 2000). More recently, such techniques to reveal surface emissivities have been supported by theoretical work (Hashimoto and Imamura, 2001; Moroz, V.I., 2002; Hashimoto, and Sugita 2003). The Venus Express PFS will obtain the first time-resolved global maps of the surface in these spectral windows.

2.5. Radiative energy balance

Radiation plays important role in various processes on the planets. It defines atmospheric temperature structure, controls photochemistry, and induces the atmospheric motions. Venus gives us examples of radiation related processes that are unique in the Solar System. First, the planet keeps absolute record in the greenhouse effect that maintains the surface temperature of ~735 K (see review by Crisp and Titov, 1997 and references therein). Second, Venus has unusual latitudinal distribution of outgoing thermal flux: receiving the solar energy at low latitudes, the planet emits considerable portion of it to space from the poles (Taylor et al., 1983; Linkin et al., 1987). This implies significant role of the atmospheric dynamics in heat transport.

Despite extensive Venus exploration in past decades, significant gaps in our knowledge of the radiation field outside and inside the atmosphere still remain. The most important open questions are the following: (1) global energy balance between the incoming and outgoing radiation; (2) distribution of heat sources in the atmosphere that drives the dynamics; (3) role of gases and aerosols and their variations in the greenhouse effect; (4) efficiency of the radiative energy escape from the lower atmosphere through the near-IR transparency windows (so called, "leaking greenhouse").

PFS onboard Venus Express will address the above mentioned problems. (1) The instrument will measure the spectrum of outgoing radiation in a broad range covering thermal and near infrared. Combined with the VIRTIS spectral measurements in the visible and UV the Venus Express mission will give full description of the radiation field escaping Venus. (2) PFS will measure the spectrum of the NIR emissions on the night side thus quantifying the efficiency of "leaking greenhouse". (3) Composition of the lower atmosphere derived from the PFS spectroscopy in the near-IR "windows" will constrain the models of the greenhouse effect. (4) Mesospheric temperature and cloud structure retrieved from the PFS measurements will be used for extensive modeling of distribution of radiative heat sources in the mesosphere in order to understand the forces driving global circulation. Further insight in the atmospheric dynamics will be obtained by comparison of the "thermal wind" field derived from PFS measurements and apparent cloud motions observed by VIRTIS and VMC instruments onboard Venus Express.

2.6. Surface

The surface of Venus is dominated by plains with a large morphological diversity, including impact craters, young volcanic features, and traces of lava fluids. There are also mountains up to 10 km elevation. The surface age is estimated at about 500 millions years. Soil composition corresponds mainly to different types of basalt.

The surface of Venus is so hot (~735 K) that even at noon on the equator its thermal radiation in 1 μm window is an appreciable part (about 10%) of the full surface brightness. The 1 μm thermal radiation from the surface of Venus penetrates through the clouds. It was detected on the night side from the Earth (Lecaucheux et al., 1993; Meadows and Crisp, 1996), and also in the experiments on Galileo (Carlson et al., 1991) and Cassini (Baines et al., 2000) spacecraft during their Venus flyby. Clouds attenuate this radiation but add nothing to it because of their low temperature.

Mapping of the surface in the 1 μm window from an orbiter is possible. However there are three problems

linked with the transfer and reflections of the surface thermal radiation by the clouds:

(1) clouds reflect some part R_c (about 80%) of upwelling thermal radiation in the 1 μm window, and transmit the part $t_c = 1-R_c$. This value depends on local optical depth of the clouds. So it would not be easy to distinguish between the variations of surface brightness and cloud optical depths. Possibly, imaging of the night side in several (minimum 2) windows could solve this problem and separate surface brightness and cloud variations. The second window should be selected in the part of spectrum dominated by an atmospheric radiation;
(2) The second problem is the multiple scattering of upwelling radiation within the clouds. It spreads the image. The size of the spot created by this spread must be equal approximately to double the height of the MCD above the surface. This is about 100 km, so NIR surface imaging from orbiters will not be able to provide a spatial resolution better than that;
(3) multiple reflections between surface and clouds. It was shown (Moroz, 2002) that it leads to low sensitivity of measured brightness to emissivity of the surface.

Finally, measurements of outgoing night emission at 1.02 μm can provide information about the surface temperature but not emissivity horizontal variations. The temperature must vary from place to place due to topography. The thermal gradient in the atmosphere is 7.5–8K/km (Seiff et al., 1985; Linkin et al., 1987; Meadows and Crisp, 1996). In this case the height difference 100 m will lead to the 2% difference in $B_P(T_s)$ value for $\lambda = 1.02$ μm. So the surface imaging in 1 μm window can give information about topography.

Surface and near-surface thermal and compositional measurements by PFS will help Venus Express for the first time reveal crucial geological, dynamical, and chemical links between the hot, pressurized surface and the overlying chemically reactive atmosphere. In particular, PFS will observe: (1) the near-surface atmospheric lapse rate and its spatial/temporal variability; and (2) the chemical, dynamical, and thermal effects of active volcanism—if present—on the atmosphere and surface.

2.6.1. Surface atmospheric lapse rate

Direct measurement of temperature lapse rates in the planetary boundary layer (0–12 km) are limited to localized measurements by the Vega 2 probe (Linkin et al., 1987) and the Venera 8–10 probes (Avduevskiy et al., 1983). More recent ground-based near-IR spectral studies (Meadows and Crisp, 1996) suggest that the lapse rate may vary considerably over the planet. In particular, measurements of the Beta Regio region indicate that the lower atmosphere is remarkably subadiabatic, with a lapse rate of 7.5 K/km vs. the expected 8.3 K/km adiabatic rate. Conversely, theoretical considerations (Dobrovolskis, 1993) indicate that the atmosphere could be statically unstable and turbulent in places, due to the influence of topography on atmospheric winds and small yet significant variations in surface heating caused by variations in slope, surface emissivity/conductivity, and latitude. Pettengill et al. (1996) noted that the critical altitude at which the Venus highlands show low radar emissivity increases by 1.5 km from the equator to high northern latitudes, perhaps reflecting a latitudinal variation in the atmospheric lapse rate. Measurements of the vertical lapse rate and/or horizontal and temporal gradients would directly address Pettengill's hypothesis as well as enable evaluations of mechanical surface weathering due to entrainment of particles in turbulent surface winds (e.g., Dobrovolskis, 1993).

Observations by NIMS (Carlson et al., 1991; Carlson et al., 1993, cf., Fig. 1, panel C), Cassini/VIMS (Baines et al., 2000) and ground-based observers (Lecacheux et al., 1993; Meadows et al., 1992; Meadows and Crisp, 1996) in the 0.85-, 0.90-, 1.01-, 1.10-, and 1.18-μm windows detect thermal emissions from the surface of Venus. Following Meadows and Crisp (1996), PFS will correlate 1-μm flux measurements with Magellan-derived surface topography to obtain constraints on thermal profiles from 0 to ~12 km altitude. The degree of near-surface static stability will be ascertained by the thermal gradient measured on mountain slopes (Ishtar Terra in the northern polar region, Beta Regio at mid latitudes, Aphrodite at low latitudes). Temporal variations in surface flux will be used to discriminate the transient effects of dynamics from the thermal emissivity of surface materials.

PFS will produce greatly enhanced coverage and increased thermal accuracy compared to Earth-based measurements, which, due to the Venus-Earth orbital resonance, are restricted to a small range of longitudes every 18 months. PFS surface temperature observations will determine the lapse rate up to ~12 km altitude, while providing improved spatial resolution (~50–100 km over the north polar region compared to ~250 km from terrestrial observatories), and much more comprehensive spatial and temporal sampling and coverage.

2.6.2. Volcanism

Magellan crater counts indicate that the surface of Venus is geologically young (~500–1000 million years). This, and the presence of a highly reactive sulfuric-acid cloud cover with a mean lifetime of 2 million years (e.g., Fegley et al., 1997), suggests the possibility of current volcanic activity. PFS will readily observe volcanic activity by its above-average thermal flux, enhanced gaseous absorptions, and increased atmospheric scattering/ absorption from ejected dust plumes. Such data will be immensely useful in characterizing the role volcanism plays in climate change and stability and in assessing the character of interior processes within a dry planet. Chemical weathering of high-dielectric-constant surface material generated by volcanism—e.g., perovskite minerals, pyrite, and pyrrho-

tite—may be observed as a spatially and temporally localized change in surface radiation. Laboratory studies under simulated Venusian conditions of iron sulfide chemical weathering (Fegley et al., 1997) have revealed that FeS_2 and Fe_7S_8 decompose in time scales of weeks to years. At high elevations, high-dielectric materials are ubiquitous at microwave wavelengths (e.g., Pettengill et al., 1988; Pettengill et al., 1992; Klose et al., 1992). PFS will globally map surface thermal emissions within the five surface-detection windows from 0.85- to 1.18-μm (cf., Baines et al., 2000). These observations will be correlated with extant radar-determined surface emissivity and elevation maps, to look for compositional differences among surface basalts (e.g., the relative distribution of silicates and sulfides, as demonstrated theoretically by Hashimoto and Sugita (2003), and more exotic volcanic deposits and high-elevation materials.

Any temporal/spatial change in the H_2O and HDO abundances associated with volcanic activity would help clarify the long-term evolution of both the atmosphere and the solid planet. As noted earlier, the observed atmospheric D/H ratio is ~150 times greater than the telluric ratio (deBergh et al., 1991; Donahue and Hodges 1993). PFS measurements of magmatic water and HDO released in a volcanic eruption would yield valuable insights into the evolution of the H_2O-poor atmosphere and the efficacy of present theories of global tectonics, insights into volcanic activity, and constraints on the oxidation rate of Venus' crust.

2.7. Chemistry, evolution, and the stability of the atmosphere of Venus

The evolution of the atmosphere of Venus has taken a different path than Mars due to the runaway greenhouse effect on the former. As a result,water is much less abundant in the Venus atmosphere and the D/H ratio is much greater than on Mars.

PFS will yield important constraints on the abundance of HDO, a key to understanding the evolutionary history of the Venusian atmosphere. Due to a variety of suspected endogenic and exogenic processes—including the effects of cometary bombardments, the solar wind, and the runaway greenhouse effect—the atmosphere of Venus today is vastly different from that at Venus' formation. The large ratio of deuterium to hydrogen in H_2O—some 150 times that found on Earth—attests to the loss of most of the water on Venus during its evolution. The mechanisms responsible for the higher D/H ratio are currently controversial and range from the loss of a primordial ocean to steady state mechanisms, wherein H_2O supplied by cometary infall and volcanic outgassing is lost by atmospheric H_2 escape and oxidation of Fe-bearing crustal minerals (Grinspoon, 1993). The size of the initial water inventory is also quite uncertain, with estimates ranging between the equivalent of 5 and 500 m of liquid water. The large uncertainty arises from a lack of precise measurements of the D/H ratio, as well as uncertainties in the current loss rate of H and O.

A particularly good diagnostic is the HDO/H_2O ratio and its variation with altitude. PFS will make this measurement, using nadir views as well as limb scans and occultations. Measurements of H_2O and HDO acquired simultaneously by PFS are expected to yield direct constraints on the D/H ratio at altitudes below ~100 km. A comparison of this result with that deduced from UV airglow measurements of the SPICAV instrument onboard Venus Express will help to determine the homopause level, and hence the eddy diffusion coefficient in a robust manner. In turn, the latter will place stringent constraints on photochemical models that are central to understanding: (1) the chemical cycles that regulate and maintain stable levels of the atmospheric species and the atmosphere as a whole; and (2) the atmospheric loss rates.

The long-term stability of the 90-bar CO_2 atmosphere is also still a mystery since CO_2 can be destroyed by photolysis ($\lambda \leqslant 0.250\,\mu m$) on a relatively short time scale, and since the products (CO and O) do not combine to recycle CO_2. Indeed, all CO_2 in the Venus atmosphere can be destroyed in 5 million years. Whereas on Mars the hydroxyl radicals (OH) are believed to play a critical catalytic role in maintaining the stability of CO_2 there (by recycling CO and O or CO and O_2 (formed upon O + O recombination) into CO_2), this mechanism fails on Venus. This is due to the relatively small mixing ratio of water vapor and an efficient removal of the HO_x along with the depletion of O_2 in the process of formation of the hygroscopic sulfuric acid ($2SO_2 + 2H_2O + O_2 \rightarrow 2H_2SO_4$) in the Venusian atmosphere. It has been suggested that chlorine in the Venus atmosphere might play a catalytic role similar to OH in the Martian atmosphere (Yung and DeMore, 1982). If that is the case, models predict the presence of several critical chlorine compounds in the atmosphere of Venus, including ClCO, $ClCO_3$, ClOO, ClO, HCl, and Cl_2. Note that chlorine would also participate in the sulfur chemistry, producing a number of species, the most abundant of which is expected to be sulfuryl chloride (SO_2Cl_2) at the ppm level.

PFS will be used to detect and measure the abundances of many diagnostic species, including several of these chlorine and sulfur species. PFS data will also be used to determine associated vertical mixing information. The results will be used in physico–photochemical–thermochemical models to understand the present state of chlorine, sulfur, and water chemistry and to develop detailed models of the evolution, climatology, and the stability of the atmosphere of Venus (cf., Atreya, 1986; Wilson and Atreya, 2003).

2.7.1. Chemistry, composition, and transport

PFS will produce time resolved global maps of the abundances of reactive species, to diagnose chemical and dynamical processes throughout the upper, middle and lower atmospheres. Venus' atmospheric chemistry involves

complex and varied chemical cycles—H_2SO_4 cloud formation from H_2O and SO_2, CO generated by photochemistry, OCS and HCl produced by thermochemistry, and SO_2, H_2O, and HCl in volcanic gases. All of these gases are measured by PFS (cf. Table 2).

Spatial variability of H_2O vapor above the cloudtops was detected by PVO/VORTEX (Schofield et al., 1982). On the nightside, the H_2O abundance was below the detection limit (6 ppm). The equatorial mid-afternoon was the wettest (up to 100 ± 40 ppm vs. <6–30 ppm elsewhere). This enhancement may have been associated with vertical uplift of deeper, moister air via convection and Hadley circulation.

3. Instrument description

3.1. Introduction

PFS is a double pendulum interferometer working in two wavelength ranges (0.9–6, and 6–45 μm). Venus radiation is divided in two beams by a dichroic mirror. The two ranges also correspond to two planes one on top of the other, in which the two interferometers are placed, so that the same motor can simultaneously move the two pendulum and the two channels are sampled simultaneously and independently. The pendulum motion is accurately controlled by means of a laser diode reference channel making use of the same optics as for Venusian radiation. The same laser diode also generates the sampling signal for the A/D converter, measuring in this way displacements of the double pendulum mirror of 450/4 nm. The measurements obtained are double sided interferograms, so that FFT can be computed without caring much about the zero optical path difference location.

3.2. Technical description

The flight hardware of the experiment is divided in four parts which we call modules, and in the connecting cables. The 4 parts are: the interferometer, with its optics and proximity electronics, which is the core of the experiment, and is called Module O. The pointing device, which allows to receive radiation from Venus or from the in flight calibration sources, which is called Module S. The Digital electronics, including a 32 Mbit mass memory, called Module E. The Power Supply, Module P, with the DC/DC converter, the redundancies, and the galvanic separated power for the 16 bits A/D converters.

3.2.1. Optical scheme of PFS–O

The optical scheme of PFS is shown in Fig. 6. The incident IR beam falls onto the entrance filter that separates the radiation of SW channel from the LW channel and directs each into the appropriate interferometer channel. The scanner in front of the interferometer allows the FOV to be pointed along and laterally to the projection of the flight path onto the Martian surface. It also directs the FOV at internal black body sources diffusers and to the open space for in-flight calibration. Each PFS channel is equipped with a pair of retroreflectors attached by brackets to an axle angularly moved by a torque motor. The axle and the drive mechanism are both used for both channels that are positioned on top of each other. The optical path difference is generated by the angular movement of the retroreflectors (Hirsch and Arnold, 1993). The controller of the torque motor uses the outputs of two reference channels, which are equipped with laser diodes. This interferometer design is very robust against slight misalignment in harsh environment compared with the classical Michelson-type interferometer

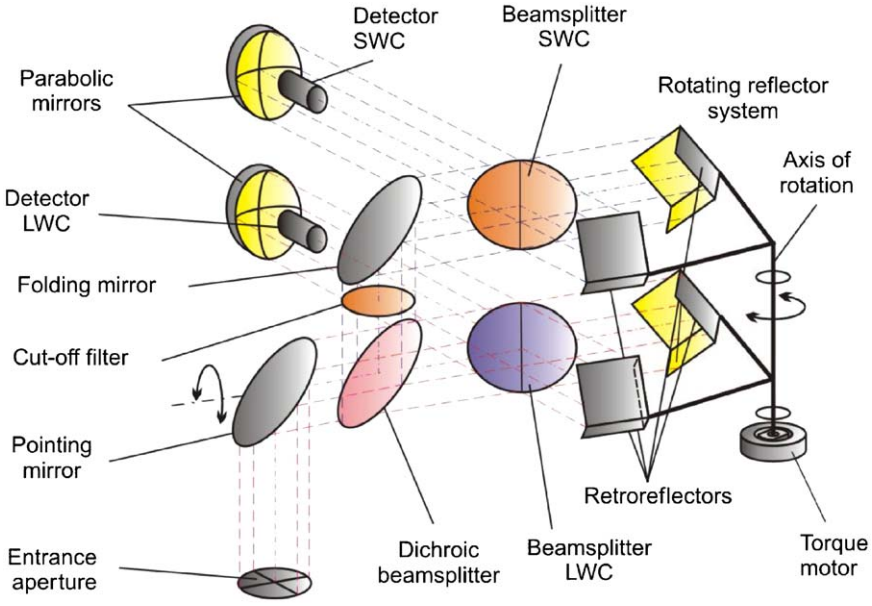

Fig. 6. The optical scheme of PFS.

(Hirsch, 1997). The detectors are placed in the center of the parabolic mirrors. The optical path is changed rotating the shaft of the double pendulum along its axis. In this way the optical path will be 4 times greater than a single cube corner displacement since two mirrors move at the same time. The dichroic mirror acts as a fork which divides the two spectral ranges. Indeed it is able to reflect all the wavelengths lower than 5 μm and remaining more or less transparent for higher wavelengths. The band stop for wavelengths lower than 0.9 μm is provided by the coated window, having a cutoff at 0.9 μm and placed in the optical inlet of the SW channel; this filter is tilted by 1.5° in order for the radiation going back to the source not to be partially reflected on the detector.

The double pendulum axis rotates by means of a brushless motor (two for redundancy) that does not experience any kind of mechanical friction. Thus the shaft of the double pendulum is sustained just by two preloaded ball bearings at very low friction. An additional mechanical friction instead is added for the purpose of a better stability of the pendulum speed.

If we place the zero optical path difference in the center of the mirror displacement, we can acquire double sided interferograms. A double sided interferogram has several advantages, among which a relative insensitivity to phase errors that otherwise should be corrected. A bilateral operation is adopted in order to reduce the time cycle of each measure but a separated calibration for each direction is recommended in order to maintain the prefixed radiometric accuracy.

The reference beam acting as spectral reference is a diode laser (InGaAsP at 900 nm) and its detector is an infrared photodiode having the maximum responsivity at about 1.2 μm. The beam of the reference channel is processed like the input signal so that the optical path of the reference is exactly coincident with the optical path of the signal to be studied. Moreover each channel has its own reference beam and a different length of the double pendulum arms is fully allowed and compensated. Because the beam splitter of the long wavelength channel is not transparent at the wavelength of the corresponding diode laser used as reference, a special small window was done during the manufacturing of it in order to keep negligible the attenuation of the laser beams through the beam splitter itself. The output beams unused of the two reference channels terminate into optical traps.

3.2.2. *The pointing mirror*

The pointing system is certainly necessary to have a complete set of measurements, since we need to measure not only the Venus radiation, but also the calibration black body and the empty space. The directions in which the mirror can be pointed are: internal calibration lamp (ICL), internal black body (IBB), deep space = 80 (DS), 25, 12.5, 0, −12.5, −25. An "imaging mode" has also been introduced, in which 11 positions of the mirror are assumed and for each position a number n (programmable) of measurements can be taken. The 11 positions are: 0°, ±2.5°, ±5.0°, ±7.5°, ±10.0, ±12.5°.

3.2.3. *In flight calibration*

During the observation session on the Venus orbit PFS periodically performs calibrations by sending commands to the Scanner to point sequentially to following calibration sources: deep space, the internal black body and the calibration lamp.

The housekeeping information obtained from module O after each calibration measurement contains, in particular,

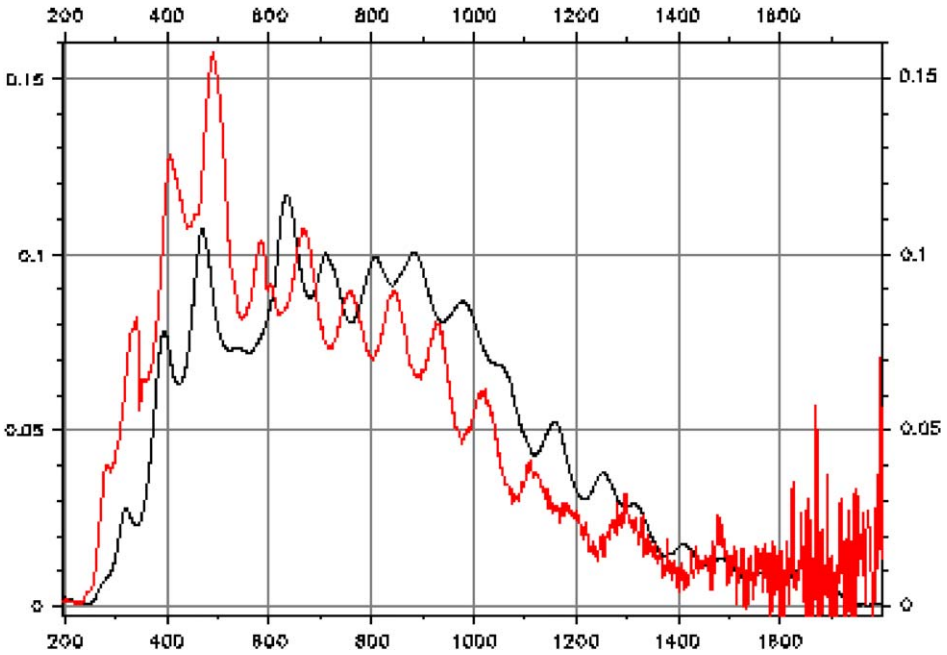

Fig. 7. PFS LW channel responsivity for MEX (red curve) and for VEX (black curve).

temperatures of sensors and the black body. These data are used for the computation of the absolute spectra for the LW channel.

4. PFS calibration results

4.1. Responsivity and signal to noise ratios

With the term "calibration" we mean here a sequence of laboratory studies of the properties of instrument, that are necessary (although may be not sufficient) to extract spectra in absolute units from future observations of Venus with PFS. In the ideal case calibrations should result in the algorithm of transfer from telemetric information to spectra of Venus in absolute units. However instrument properties are not constant in time, and also the problem is complicated by the differences between laboratory and space conditions. Some additional information including in-flight calibration and even models of Venusian radiation spectra will be necessary for the real processing of measured data.

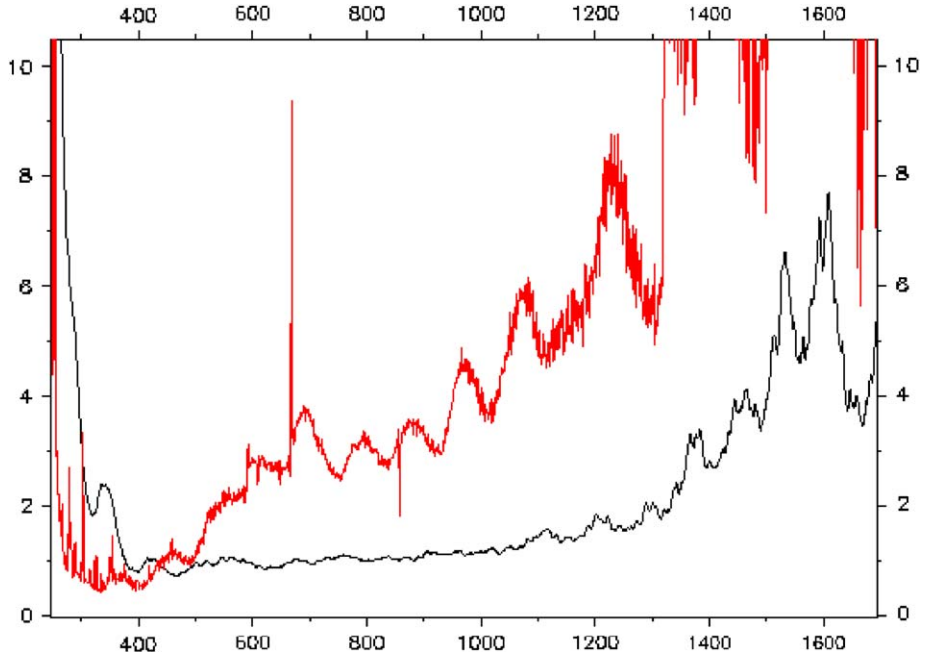

Fig. 8. NER for the LW channel of PFS for MEX (red curve) and VEX (black curve).

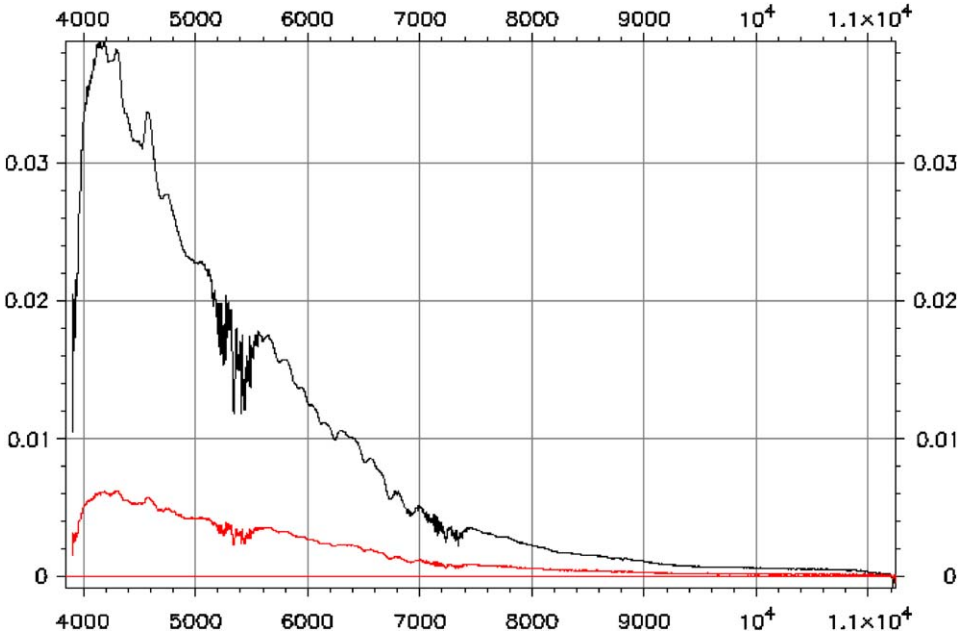

Fig. 9. Responsivity of the solar part of the SW channel of PFS–VEX in the two modes: dayside (red curve) and night side (black curve).

Having a set of n independently found $B_{v0}(i)$ spectra we can compute the average spectrum B_{v0} and Noise equivalent brightness

$$\mathrm{NEB}_v = \left\{\Sigma\left[(B_{v0}(i) - B_{v0})^2\right]/(n-1)\right\}^{0.5}.$$

A more detail discussion of processing procedure for IR spectrometers data is given in the book by Hanel et al. (1992). Two Blackbody imitator sources (cooled by liquid nitrogen) were used to study the PFS LW-channel properties. An integrating sphere source and one blackbody at 1400 K were used to study the PFS SW channel. Sensitivity D_v and noise equivalent brightness NEB_v were then computed from these measurements. The spectral resolution was measured with a mercury lamp and by taking some spectra with known features.

Rough computations show that SNR at Venus of about 100 or larger will be achieved in vicinity of 15 μm bands by

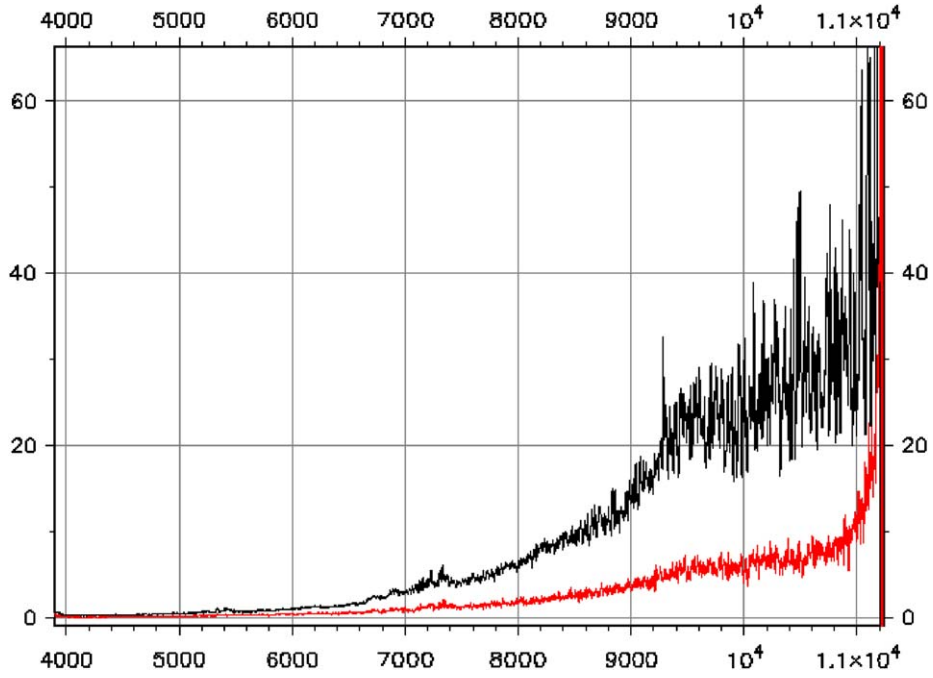

Fig. 10. NER of PFS SW channel in the solar part: dayside mode (black curve) and nightside mode (red curve).

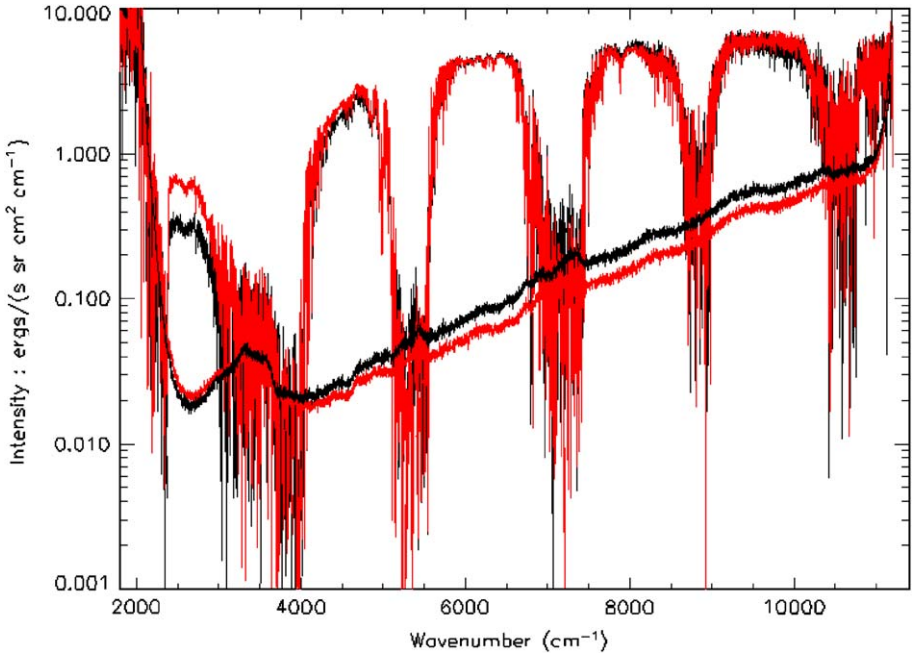

Fig. 11. SW spectrum of the Earth's atmosphere looking out of the window: black curve dayside mode, red curve night side mode. The oblique curve gives the NER.

$T = 220$ K (see Fig. 7) similar or better than the PFS LW channel on Mars Express. This is enough good for retrievals of the vertical temperature profiles of the Venusian atmosphere. In any case a further study of the thermal behavior of the instrument is necessary and will be done in space. It is evident from Fig. 8 that the NER for the PFS LWC VEX has been reduced with respect to the MEX case, and this is probably due to the better performance of the beam splitter.

The responsivity of the SW channel is given in Fig. 9 for the solar part. The NER is given in Fig. 10. In both figures two curves are given: one for dayside mode and one for night side mode (different attenuation or gain factors). From Fig. 9 it seems that for wavenumbers $v > 8000\,\mathrm{cm}^{-1}$

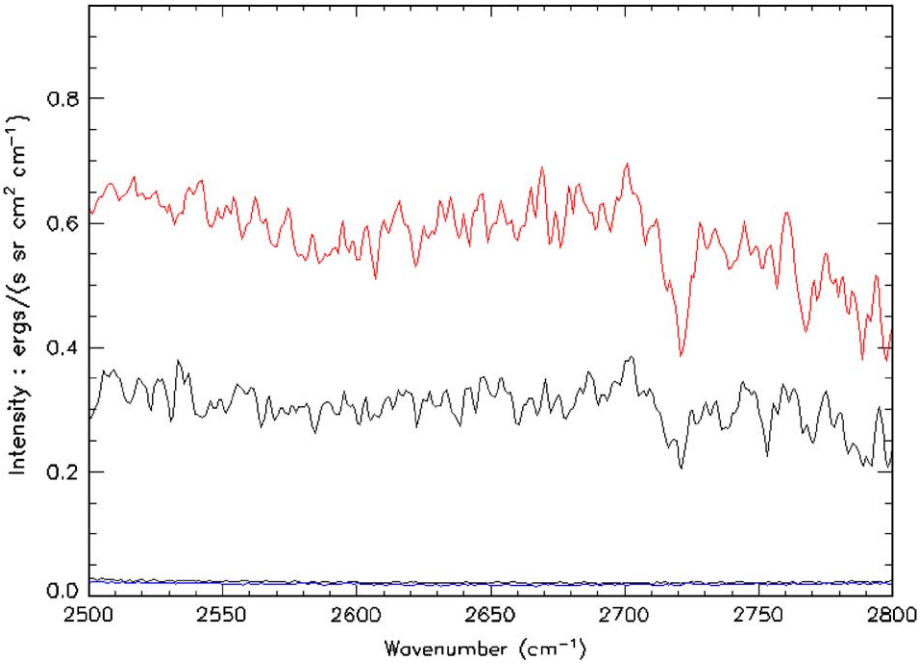

Fig. 12. PFS measurements looking out of the window: HDO line. Red curve is nightside mode, black is dayside mode.

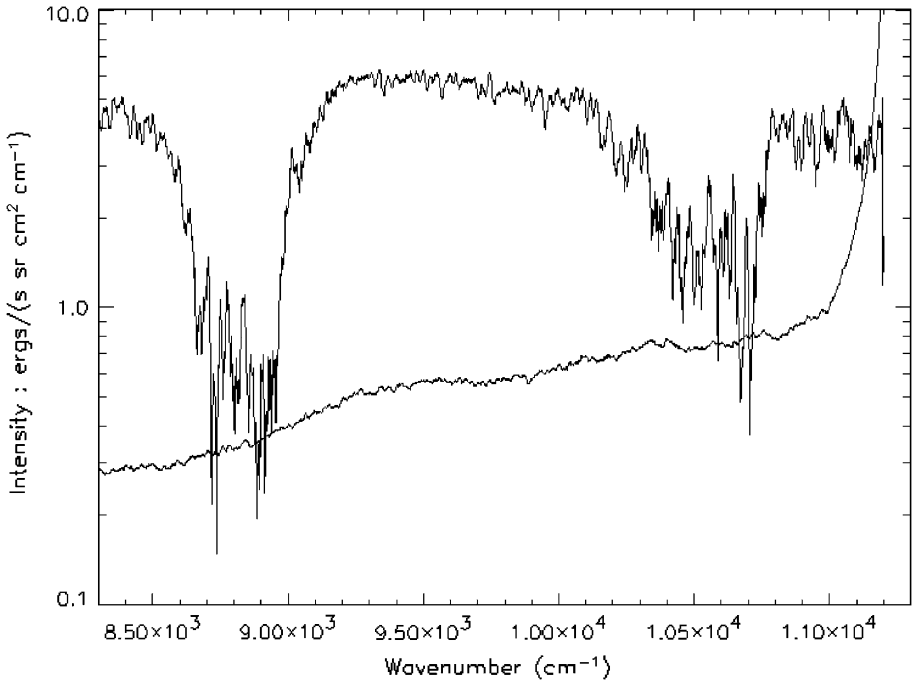

Fig. 13. Blow up of the Fig. 11 in a spectral region not available on PFS–MEX. Two new water bands are observed. Data are smoothed over 15 points.

the responsivity is rather poor, the reason is that the semitransparent mirror separating LW and SW radiation has too low reflectivity in this part of spectra, and also this is the part of the spectrum in which losses in optical alignement are more effective. In reality the situation is much better than it appears from Figs. 9 and 10. In order to test the actual performance we have used the PFS VEX for measurements in the laboratory, looking out of the window and measuring the spectrum of the Earth's atmosphere. The data are presented in the next paragraph.

4.2. Samples of performed measurements

We demonstrate the performance of PFS also by showing some measurements made in the laboratory in order to test the entire range of wavenumbers covered by PFS. Measurements were made by looking out of the open window of the institute in the direction of distant mountains. Measurements were made at room temperature. Fig. 11 gives the measured spectrum from 2000 to 11400 cm^{-1}. Data were acquired in two different modes: dayside mode (attenuation of the signal by a factor 8, and nightside mode amplification by 8). The data are calibrated. The measured NER is also shown in the figure separately for the two measurements. Enlarged parts of these spectra are given in Fig. 12 for the HDO line and Fig. 13 for the spectral interval added for PFS–VEX and absent in PFS–MEX namely 8000–11400 cm^{-1}. These measurements show that by averaging of a few measurements, the SNR can be increased in order to achieve successfully all the scientific objectives.

References

Allen, D.A., Crawford, J.W., 1984. Cloud structure on the dark side of Venus. Nature 307, 222–224.

Atreya, S.K., 1986. Atmospheres and Ionospheres of the Outer Planets and Their Satellites. Springer, New York, Berlin, pp. 93–95, 82–88 (Chapter 5).

Avduevskiy, V.S., Marov, M.Y., Kulikov, Y.N., Shari, V.P., Gorbachevskiy, A.Y., Uspenskiy, G.R., Cheremukhina, Z.P., 1983. Structure and parameters of the Venus atmosphere according to Venera probe data. In: D. Hunten, M., Collin, L., Donahue, T.M., Moroz, V.I. (Eds.), Venus. University of Arizona Press, Tucson, pp. 681–765.

Baines, K.H., Bellucci, G., Bibring, J.-P., Brown, R.H., Buratti, B.J., Bussoletti, E., Capaccioni, F., Cerroni, P., Clark, R.N., Cruikshank, D.P., Drossart, P., et al., 2000. Detection of sub-micron radiation from the surface of Venus by Cassini/VIMS. Icarus 148, 307–311.

Bézard, B., deBergh, C., Crisp, D., Maillard, J.-P., 1990. The deep atmosphere of Venus revealed by high-resolution nightside spectra. Nature 345, 508–511.

Carlson, R.W., Baines, K.H., Encrenaz, F.W., Drossart, P., Kamp, L.W., Pollack, J.B., Lellouch, E., Collard, A.D., Calcutt, S.B., et al., 1991. *Galileo* infrared imaging spectroscopy measurements at Venus. Science 253, 1541–1548.

Carlson, R.W., Baines, K. H., Girard, M., Kamp, L.W., Drossart, P., Encrenaz, T., Taylor, F.W., 1993. Galileo/NIMS near infrared thermal imagery of the surface of Venus, Proceedings of the XXIV Lunar and Planetary Science Conference, p. 253.

Connes, P., Noxon, J.F., Traub, W.A., Carleton, N.P., 1979. O_2 ($^1\Delta$) emission in the day and night airglow of Venus. Astrophys J. 233, L29–L32.

Crisp, D., Titov, D.V., 1997. The thermal balance of the Venus atmosphere. In: Bougher, S.W., Hunten, D.M., Phillips, R.J. (Eds.), Venus II. The University of Arizona Press, Tucson, Arizona, pp. 353–384.

Crisp, D., Sinton, W.M., Hodapp, K.W., Ragent, B., Gerbault, F., Goebel, J., Probst, R., Allen, D., Pierce, K., 1989. The nature of the near-infrared features on the Venus night side. Science 253, 1263–1267.

Crisp, D., Allen, D., Grinspoon, D.H., Pollack, J.B., 1991. The dark side of Venus: near-infrared images and spectra from the Anglo-Australian Observatory. Science 253, 1263–1267.

de Bergh, C., Bézard, B., Owen, T., Crisp, D., Maillard, J.-P., Lutz, B.L., 1991. Deuterium on Venus: observations from Earth. Science 251, 547–549.

Dobrovolskis, A.R., 1993. Atmospheric tides on Venus. IV. Topographic winds and sediment transport. Icarus 103, 276–289.

Donahue, T.M., Hodges, R.R., 1993. Venus methane and water. Geophys. Res. Lett. 20, 591–594.

Fegley, B., Zolotov, M.Yu., Lodders, K., 1997. The oxidation state of the lower atmosphere and surface of Venus. Icarus 125, 416–439.

Formisano, V., Angrilli, F., Arnold, G., Atreya, S., Bianchini, G., Biondi, D., Blanco, A., Blecka, M.I., Coradini, A., Colangeli, L., Ekonomov, A., Encrenaz, T., Esposito, F., Fonti, S., Giuranna, M., Grassi, D., Gnedykh, V., Grigoriev, A., Hansen, G., Hirsh, H., Khatuntsev, I., Kiselev, A., Ignatiev, N., Jurewicz, A., Lellouch, E., Lopez Moreno, J., Marten, A., Mattana, A., Maturilli, A., Mencarelli, E., Michalska, M., Moroz, V., Moshkin, B., Nespoli, F., Nikolsky, Y., Orfei, R., Orleanski, P., Orofino, V., Palomba, E., Patsaev, D., Piccioni, G., Rataj, M., Rodrigo, R., Rodriguez, J., Rossi, M., Saggin, B., Titov, D., Zasova, L., 2005. The planetary fourier spectrometer (PFS) onboard the European Mars Express Mission. Planet Space Sci. vol. 53, 963.

Grinspoon, D.H., Pollack, J.B., Sitton, B.R., Carlson, R.W., Kamp, L.W., Baines, K.H., Encrenaz, Th., Taylor, F.W., 1993. Probing Venus's cloud structure with Galileo-NIMS. Planet. Space. sci. 41, 515–542.

Hashimoto, G.L., Imamura, T., 2001. Elucidating the rate of volcanism on Venus: detection of lava eruptions using near-infrared observations. Icarus 154, 239–243.

Hashimoto, G.L., Sugita, S., 2003. On observing the comnpositional variability of the surface of Venus using nightside near-infrared thermal radiation. JGR-Planets 108 (E9), 5109.

Klose, K.B., Wood, J.A., Hashimito, A., 1992. Mineral equilibria and the high reflectivity of Venus mountaintops. J. Geophys. Res. 97, 16353–16369.

Lecaucheux, J.A., Drossart, P., Laques, P., Deladrierre, F., Colas, F., 1993. Detection of the surface of Venus on 1 μm from ground based observations. Planet. Space Sci. 41, 543–550.Limaye, S.S., Suomi, V.E., 1981. Cloud motions on Venus: global structure and organization. J. Atmos. Sci. 38, 1220–1235.

Linkin, V.M., Blamont, J., Devyatkin, S.I., Ignatova, S.P., Kerzhanovich, V.V., Lipatov, A.N., Malik, K., Stadnyk, B.I., Stolyarchuk, Ya.V., Sanotskii, P.G., Terterashvili, A.V., Frank, G.A., Khlyustova, L.I., 1987. Thermal structure of the atmosphere of Venus from the results of measurements taken by landing vehicle Vega-2. Cosmic Res. 25, 501–512.

Meadows, V.S., Crisp, D., Allen, D.A., 1992. Groundbased near-IR observations of the surface of Venus. Int. Colloq. Venus LPI Contribution 789, 70–71.

Meadows, V.S., Crisp, D., 1996. Ground-based near infrared observations of the Venus nightside: the thermal structure and water abundance near the surface. J. Geophys. Res. 101, 4595–4622.

Moroz, V.I., 1981. The atmosphere of Venus. Space Sci. Rev. 29, 3–127.

Moroz, V.I., 2002. Estimates of visibilities of the surface of Venus from descent probes and balloons. Planet. Space Sci. 50, 287–297.

Pettengill, G.H., Ford, P.G., Chapman, B.D., 1988. Venus: surface electromagnetic properties. J. Geophys. Res. 93, 14881–14892.

Pettengill, G.H., Ford, P.G., Simpson, R.A., 1996. Electrical properties of the Venus surface from bistatic radar observations. Science 272, 1628–1631.

Pettengill, G.H., Ford, P.G., Wilt, R.J., 1992. Venus surface emission as observed by Magellan. J. Geophys. Res. 97, 13091–13102.

Pollack, J.B., et al., 1993. Night infrared light from Venus' night side: a spectroscopic analysis. Icarus 103, 1–42.

Schofield, J.T., Taylor, F.W., McCleese, D.J., 1982. The global distribution of water vapor in the middle atmosphere of Venus. Icarus 52, 263–278.

Seiff, et al., 1985. Models of the structure of the atmosphere of Venus from the surface to 100 kms altitude. In: Kliore, A.J., Moroz, V.I., Keating, G.M., (Eds.), The Venus Reference Atmosphere. (Adv.Space Res. 5, N 11, pp. 3–58).

Spankuch, D., et al., 1985. Infrared experiment on VENERA-15 and VENERA-16 orbiters. two. Preliminary results of the temperature profiles retrieval. Kosmicheskie issledovanija 23, 206–220 (in Russian).

Taylor, F.W., Hunten, D.M., Ksanfomality, L.V., 1983. The thermal balance of the middle and upper atmosphere of Venus. In: Hunten, D.M., Colin, L., Donahue, T.M., Moroz, V.I. (Eds.), Venus Hunten. The University of Arizona Press, Tucson, Arizona, pp. 650–680.

Taylor, F.W., Crisp, D., Bezard, B., 1997. Near infrared sounding of the lower atmosphere of Venus. In: Bougher, S.W., Hunten, D.M., Phillips, R.J. (Eds.), Venus II. The University of Arizona Press, Tucson, Arizona, pp. 325–352.

Twomay, S., Herman, D., Rabinoff, R., 1977. An extention of Chahine method of inverting the radiative transfer solution equation. J. Atmos. Sci. 34, 1085.

Von Zahn, U., Kumar, S., Niemann, N., Prinn, R., 1983. Composition of the Venus atmosphere. In: Hunten, D.M., Colin, L., Donahue, T.M., Moroz, V.I. (Eds.), Venus. The University of Arizona Press, Tucson, Arizona, pp. 299–430.

Von Zahn, U., Moroz, V.I., 1985. Composition of the Venus atmosphere below 100 km altitude. In: Kliore, A.J., Moroz, V.I., Keating, G.M. (Eds)., (Adv.Space Res. 5, N 11, pp. 173–196).

Wilson, E.H., Atreya, S.K., 2003. Chemical sources of haze formation in Titan's atmosphere. Planetary and Space Science 52, 1017–1033.

Yung, Y.L., DeMore, W.B., 1982. Photochemistry of the stratosphere of Venus: implications for atmospheric evolution. Icarus 51, 197–212.

Zasova, L.V., Khatountsev, I.V., Moroz, V.I., Ignatiev, N.I., 1999. Structure of the Venus middle atmosphere: Venera 15 IR Fourier spectrometry data revisited. Adv. Space Res. 23 (N 9), 1559–1568.

Zasova, L.V., Moroz, V.I., Formisano, V., Ignatiev, N.I., Khatuntsev, I.V., 2004. Infrared spectrometry of Venus: IR Fourier spectrometer on Venera 15 as a precursor of PFS for Venus Express. Adv. Space Res. 34, 1655–1667.